



Universiteit
Leiden
The Netherlands

Experimental test of a fluctuation-induced first-order phase transition: The nematic-smectic-A transition

Anisimov, M.A.; Cladis, P.E.; Gorodetskii, E.E.; Huse, D.A.; Podneks, V.E.; Taratuta, V.G.; ... ;
Voronov, V.P.

Citation

Anisimov, M. A., Cladis, P. E., Gorodetskii, E. E., Huse, D. A., Podneks, V. E., Taratuta, V. G.,
... Voronov, V. P. (1990). Experimental test of a fluctuation-induced first-order phase
transition: The nematic-smectic-A transition. *Physical Review A*, 41(12), 6749-6762.
doi:10.1103/PhysRevA.41.6749

Version: Not Applicable (or Unknown)

License: [Leiden University Non-exclusive license](#)

Downloaded from: <https://hdl.handle.net/1887/68139>

Note: To cite this publication please use the final published version (if applicable).

Experimental test of a fluctuation-induced first-order phase transition: The nematic–smectic- A transition

M. A. Anisimov

Moscow Oil and Gas Institute, 65 Leninski Prospect, Moscow 117917, U.S.S.R.

P. E. Cladis

AT&T Bell Laboratories, Murray Hill, New Jersey 07974

E. E. Gorodetskii

Moscow Oil and Gas Institute, 65 Leninski Prospect, Moscow 117917, U.S.S.R.

David A. Huse

AT&T Bell Laboratories, Murray Hill, New Jersey 07974

V. E. Podneks

Moscow Oil and Gas Institute, 65 Leninski Prospect, Moscow 117917, U.S.S.R.

V. G. Taratuta

Massachusetts Institute of Technology, Cambridge, Massachusetts 02139

Wim van Saarloos

AT&T Bell Laboratories, Murray Hill, New Jersey 07974

V. P. Voronov

Moscow Oil and Gas Institute, 65 Leninski Prospect, Moscow 117917, U.S.S.R.

(Received 18 September 1989)

In 1974, Halperin, Lubensky, and Ma (HLM) [Phys. Rev. Lett. **32**, 292 (1974)] predicted that the nematic–smectic- A transition of pure compounds and their mixtures should be at least weakly first order. One way to obtain such a prediction is to treat the smectic order parameter as a constant and integrate out the director fluctuations. The coupling between the director fluctuations and the smectic order parameter then generates a cubic term in the effective free energy for the nematic–smectic- A (N – Sm - A) transition, which tends to drive the transition first order. So far, however, there has not been clear experimental evidence in support of this prediction: Some materials appear to exhibit a first-order transition but others a second-order transition. In this paper we introduce two new approaches to test the predictions of HLM. First, we note that if a cubic term in the effective free energy for the smectic order parameter is present, its effect is dominant near the Landau tricritical point (LTP), where the quartic term in the free energy vanishes. In a mean-field approximation, a universal scaling form of the latent heat can then be derived close to the LTP. Its form depends sensitively on the presence of the cubic term. By reanalyzing earlier calorimetric measurements near the LTP, we find that these data yield evidence for the presence of the cubic term predicted by HLM. The second new approach to experimentally determine whether a transition is weakly first order or second order is a dynamical method. This general method is based on the observation that when a transition is (weakly) first order, the dynamics of interfaces are symmetric about T_c , so that an interface can propagate into both phases, depending on whether the sample is undercooled or overheated (corresponding to “melting” and “freezing”). For a weakly first-order transition, a simple scaling relation for the interface speed can be derived. In contrast, the dynamics of propagating fronts close to a second-order transition are very asymmetric. Results of moving interfaces close to T_c in 8CB-10CB (where CB represents cyanobiphenyl) and 9CB-10CB mixtures are presented and shown to support both qualitatively as well as quantitatively the prediction that the transition is always at least weakly first order. For the N – Sm - A transition in these compounds, our comparison finds that the dynamic experiments are more sensitive than the adiabatic calorimetry experiments by about one order of magnitude and more sensitive than the x-ray-diffraction experiments by about two orders in detecting the phase-transition order.

I. INTRODUCTION

A surprising phenomenon that was first predicted theoretically some 15 years ago is that fluctuations can drive a transition from second order to first order. This prediction of Halperin, Lubensky, and Ma¹ (HLM) is believed to apply both to the normal-metal–superconducting transition and the nematic (*N*)–smectic-*A* (*Sm-A*) transition in liquid crystals. Unfortunately, for type-I superconductors the first-order nature of the transition is only expected to become visible within a few μK from the transition temperature.¹ The effect therefore appears to be immeasurably small. In contrast, for the nematic–to–smectic-*A* transition (*N-Sm-A* transition) HLM estimated that the temperature range where the first-order nature of the transition is expected to manifest itself is sufficiently large to be measurable.

According to their original paper, HLM (Ref. 1) expected the normal-superconductor transition and the *N-Sm-A* transition to be *always* weakly first order. Later more detailed work by Dasgupta and Halperin² indicates, however, that somewhere in the regime of type-II superconductivity, the transition reverts to second order. Indeed, as we shall discuss, the arguments of HLM are simplest and most compelling in the extreme type-I limit: in that limit, the first-order nature of the transition becomes apparent before critical fluctuations become important, so that the superconductor order parameter can be treated in a simple mean-field approximation.

Historically, the *N-Sm-A* transition was believed to be of first order but as pointed out by Kobayashi,³ McMillan,⁴ and de Gennes⁵ in the early days of phase transitions in liquid crystals, the Landau rules for phase transitions applied to a free energy that contains only even powers of the smectic order parameter ψ , did not exclude the possibility that it could be second order.⁵ However, the effect of layering could lead to an enhancement of the orientational order in the smectic *A* phase relative to the nematic phase.^{4,5} Formally, this coupling appears as a renormalization of the coefficient of the fourth-order invariant of a Landau expansion. This is indeed observed in several studies,^{6–13} and this effect may be used to effectively “tune” the coefficient of the fourth-order invariant to reach the region near the Landau tricritical point (LTP), the point in the phase diagram where the coefficient of the fourth-order term vanishes.

The attractive feature of searching for evidence for the HLM effect at the *N-Sm-A* transition is the existence of the LTP. Near this point, the experimental signature should be clearest, while at the same time the HLM prediction is well founded and simple, since a mean-field treatment of the smectic order parameter ψ becomes possible. To understand why this is so intuitively, it is sufficient to note that at the LTP, the upper critical dimension is $d = 3$, so that (apart from logarithmic corrections) mean-field theory is essentially correct. Alternatively, one may note that approaching the LTP from the second-order side corresponds in the analogy with superconductivity to taking the limit in which the superconductor becomes of extreme type I. As noted already

above, in this limit it is justified¹ to treat the order parameter in a mean-field approximation and the analysis of HLM unmistakably leads to the prediction that the transition should be weakly first order. Indeed, as will be discussed in more detail later, the analysis of HLM implies that in this regime the effective Landau free energy for the smectic order parameter ψ contains an *additional* nonanalytic cubic term proportional to $-B|\psi|^3$, with $B > 0$, as a result of the coupling of the director field with ψ . Since $B > 0$, this cubic term makes the transition first order, regardless of the sign of the fourth-order coefficient.

In spite of many sophisticated and accurate experiments, there has not been clear experimental evidence to support the HLM predictions that the *N-Sm-A* transition is at least weakly first order near the LTP. It was found⁸ that some pure compounds and mixtures show a first-order transition, while the data on other materials were completely consistent with the phase transition being second order.

The problem with trying to settle the nature of a weakly first-order transition with calorimetric or x-ray measurements is, of course, that they can only set an upper limit on the latent heat or a lower limit on the correlation length at T_c , respectively. It is the purpose of this paper to show that additional information on the order of the *N-Sm-A* phase transition can be obtained both from a more sophisticated scaling analysis of the latent heat in the neighborhood of the LTP and from experiments on interface propagation close to the critical point. In particular, we will show that close to the LTP, a universal scaling form for the latent heat can be derived in the mean-field approximation, whose form is sensitive to the magnitude of the HLM cubic term. By reanalyzing earlier calorimetric measurement near the LTP, we find that these data *do* yield evidence for the presence of the cubic term in the free energy predicted by HLM. Our second new approach to study the order of the phase transition is a dynamical one;¹⁴ it is based on the observation that when a transition is (weakly) first order, the dynamics are symmetric about T_c , so that an interface can propagate into both phases, depending on whether the sample is undercooled or overheated; for a weakly first-order transition, a simple scaling relation for the interface speed can be derived. The dynamics of propagating fronts close to a second order transition are very asymmetric, however. As we shall see, experiments on moving interfaces in a number of mixtures provide additional *qualitative* as well as *quantitative* evidence that the *N-Sm-A* transition is indeed weakly first order near the LTP.

This paper is organized as follows. In Sec. II, we first review the results of HLM for the nematic–smectic-*A* phase transition, in order to emphasize the fact that their prediction is essentially based on the generation of a cubic term in the free energy. We then analyze the Landau free energy with a cubic term included in Sec. III. Since the susceptibility is finite at the LTP in this case, we introduce the idea of scaling it at any point on a phase transition line by its magnitude at the LTP. In this way, we find a universal curve that can be used to compare all the data. This scaling form is used in Sec. IV to reanalyze

previous measurements of the latent heat in $\overline{6}O\overline{1}0\overline{6}O\overline{1}2$, 9CB-10CB, and 8CB-10CB mixtures. We then turn to a discussion of the general ideas underlying the dynamical approach in Sec. V and discuss its application to the N -Sm- A transition in Sec. VI. A number of questions raised by our results are briefly discussed in Sec. VII.

II. HALPERIN-LUBENSKY-MA THEORY APPLIED TO THE NEMATIC-TO-SMECTIC- A PHASE TRANSITION

The N phase breaks the continuous rotational symmetry of the isotropic liquid phase in that the molecules have some average orientation given by the director \mathbf{n} . The structure of the A phase consists of layers parallel to \mathbf{n} with thickness d of the order of the molecular length,¹⁵ so that the continuous translational symmetry in the direction parallel to \mathbf{n} is broken in the A phase. When the layer normal is on average parallel to the z direction, the smectic order parameter is a complex field $\psi(\mathbf{r})$ that specifies the amplitude and phase of the density modulation $\rho(\mathbf{r}) = \rho_0 \{1 + \text{Re}[\psi(\mathbf{r})e^{iq_0 z}]\}$ induced by the layering. Here $q_0 = 2\pi/d$ is the wave vector corresponding to the layer spacing d , and the complex field $\psi(\mathbf{r})$ has its spatial variation on scales larger than d .

Since the layer normal locally wants to be parallel to \mathbf{n} , the smectic order parameter locally wants to be of the form $\psi(\mathbf{r})e^{iq_0 z} = e^{iq_0 \mathbf{n} \cdot \mathbf{r}} = e^{iq_0 z + iq_0 \delta \mathbf{n} \cdot \mathbf{r}}$ if the director field fluctuates by an amount $\delta \mathbf{n}$ about the z direction. Hence, the smectic order parameter is strongly coupled to the director field; this is reflected in the form of the free energy density¹ $f'(\psi, \delta \mathbf{n})$:

$$\begin{aligned} f'(\psi, \delta \mathbf{n}) = & \frac{1}{2} A' |\psi|^2 + \frac{1}{4} C |\psi|^4 + \frac{1}{6} E |\psi|^6 + \frac{1}{2M_{\parallel}} |\nabla_{\parallel} \psi|^2 \\ & + \frac{1}{2M_{\perp}} |(\nabla_{\perp} - iq_0 \delta \mathbf{n}) \psi|^2 \\ & + \frac{1}{2} [K_1 (\nabla \cdot \delta \mathbf{n})^2 + K_2 (\mathbf{n} \cdot \nabla \times \delta \mathbf{n})^2 \\ & + K_3 (\mathbf{n} \times \nabla \times \delta \mathbf{n})^2] . \end{aligned} \quad (1a)$$

The K_i are the bare Frank constants. Note that M_{\parallel} and M_{\perp} determine the correlation lengths ξ_{\parallel} and ξ_{\perp} parallel and perpendicular to \mathbf{n} , respectively. Odd powers of ψ do not appear in the free energy density because a change in sign $\psi \rightarrow -\psi$ just corresponds to a translation of the smectic layers by $d/2$ and because the coarse-grained free energy density has to be analytic in ψ .

In the absence of smectic layering, the long-wavelength director fluctuations are soft—their energy is proportional to k^2 , where \mathbf{k} is their wave vector. However, because of the coupling between ψ and \mathbf{n} , layering suppresses transverse director fluctuations and the strength of the long-wavelength transverse director fluctuations is ψ dependent. As a result, on averaging over the director fluctuations, the effective free energy density acquires an additional ψ dependence.

This is most easily seen if we consider a homogeneous value of ψ ($\psi = \text{const}$) and neglect the fluctuations in ψ ; moreover, we will, for simplicity, work in the one con-

stant approximation $K_1 = K_2 = K_3 = K$. In this approximation, we have upon integrating over the director fluctuations for the effective free energy $f(\psi)$

$$\frac{df(\psi)}{d|\psi|} = A' |\psi| + C |\psi|^3 + E |\psi|^5 + \frac{q_0^2}{M_{\perp}} |\psi| \langle [\delta \mathbf{n}(\mathbf{r})]^2 \rangle . \quad (1b)$$

Since the terms in f' quadratic in $\delta \mathbf{n}$ can be written as $\int d\mathbf{k} |\delta \mathbf{n}(\mathbf{k})|^2 (Kk^2 + q_0^2 \xi_{0\perp}^2 |\psi|^2)$ we get from the standard fluctuation formula for the thermally averaged director fluctuations

$$\langle |\delta \mathbf{n}(\mathbf{k})|^2 \rangle \sim \frac{1}{Kk^2 + q_0^2 \xi_{0\perp}^2 |\psi|^2} . \quad (2)$$

This expression shows that a nonzero value of the smectic order parameter opens a gap as $k \rightarrow 0$ in the spectrum of transverse director fluctuations. For $\langle [\delta \mathbf{n}(\mathbf{r})]^2 \rangle$, we now obtain

$$\begin{aligned} \langle |\delta \mathbf{n}(\mathbf{r})|^2 \rangle & \sim \int_0^{k_c} dk \frac{k^2}{Kk^2 + q_0^2 \xi_{0\perp}^2 |\psi|^2} \\ & = \frac{k_c}{K} - B' |\psi| , \quad B' > 0 . \end{aligned} \quad (3)$$

Here k_c is a microscopic cutoff wave number which we assumed is large enough that $Kk_c^2 \gg q_0^2 \xi_{0\perp}^2 |\psi|^2$. When integrating over the director fluctuations, we see from Eq. (1b) that its effect on the derivative of the effective free energy $f(\psi)$ will be through a term of the form $q_0^2 \langle [\delta \mathbf{n}(\mathbf{r})]^2 \rangle |\psi| \sim k_c |\psi| - B' |\psi|^2$. Hence, transverse director fluctuations not only induce renormalization of the coefficients A' but also lead to the introduction of a new term $-(B'/3) |\psi|^3$ in f . We thus obtain a local free energy density of the form¹⁶

$$f(\psi) = \frac{1}{2} A |\psi|^2 - \frac{1}{3} B |\psi|^3 + \frac{1}{4} C |\psi|^4 + \frac{1}{6} E |\psi|^6 . \quad (4)$$

This form of the local free-energy density will be the basis for the scaling analysis in Sec. III. Note that since the remainder of our analysis will be on the level of a mean-field approximation for which the fact that the smectic order parameter ψ is complex does not play a role, we will from now on treat ψ as a real quantity. The important feature of Eq. (4) is the presence of the cubic term that makes the phase transition necessarily first order in mean-field theory. This term is unusual in that it is non-analytic at $\psi = 0$. This nonanalytic feature arises because *all* the long-wavelength director fluctuations have been integrated out.

The above discussion illustrates the simplicity of the HLM argument^{1,17} that the N -Sm- A transition should be a fluctuation-induced first-order transition. As mentioned in the Introduction, a similar argument holds for the normal metal-superconductor transition. (The analogy between this transition and the N -Sm- A transition, discovered by de Gennes,⁵ is not perfect: only one length is needed to describe the isotropic normal metal-superconducting transition whereas the N -Sm- A transition is anisotropic and requires two coherence lengths ξ_{\parallel} and ξ_{\perp} .) Note that although this argument includes the fluctuations of \mathbf{n} , the remainder of the argument is on a

mean-field level because fluctuations of ψ are ignored. Near the LTP, a treatment on this level seems reasonable, since the upper critical dimension for the LTP is 3. We will confine our attention to this regime. In the language of superconductivity, the LTP is the limit of extreme type-I behavior, where the fluctuations in the gauge field are indeed much stronger than those of ψ so the HLM approach is again reasonable for this regime.¹ For sufficiently large C , fluctuations in ψ become more important and the HLM argument becomes questionable; here the transition may well return to being continuous, as is argued for the case of type-II superconductivity by Dasgupta and Halperin.²

On the experimental side, support for the theory of HLM has been inconclusive. Some materials show N -Sm- A transitions with immeasurably small latent heats as measured by adiabatic scanning calorimetry^{2,3} while in a number of x-ray diffraction experiments the coherence lengths showed no tendency to have finite limiting values as the transition temperature $T_{N\text{-Sm-}A}$ was approached from above.⁹ Adiabatic scanning calorimetry measurements have also been made on various mixtures that exhibit progressively smaller latent heats at progressively larger nematic ranges. Such behavior is qualitatively consistent with the existence of the LTP which should appear due to the classical coupling between the nematic and smectic results. However, as pointed out by Anisimov *et al.*,¹⁸ there is an important difference between the mean-field theoretical predictions and N -Sm- A tricritical behavior. Landau theory *without the cubic term* predicts that the latent heat L along the first-order side of the transition line should be a linear function of the distance to the tricritical point, i.e., in a mixture with concentration x ,

$$L \sim x - x^*, \quad (5)$$

where x^* is the tricritical concentration of the mixture. Experiment^{6,7} does not support this prediction in the case of the N -Sm- A transition. In the vicinity of the N -Sm- A tricritical point the concentration dependence of the latent heat appears to be nonlinear, looking approximately quadratic. In Ref. 18, it was found that such behavior was consistent with the assumption that the Landau expansion of the free energy contained a small cubic term in the vicinity of the LTP. This was the first experimental evidence supporting the predictions of the HLM theory.

In passing, we also note that at a tricritical point, one expects a specific heat exponent $\alpha = \frac{1}{2}$. However, the fact that experiments are done at fixed composition leads to an appreciable (Fisher) renormalization of the exponents. This has recently been analyzed in detail by Hill *et al.*¹⁹

Compounds with the larger nematic ranges have no measurable latent heats at the N -Sm- A transition. Only recently have the consequences of observing an interface propagating at this transition been explored.¹⁴ It was found that the N -Sm- A transition was first order even in compounds with no measurable latent heat at this transition. We will show that these measurements are indeed consistent with the existence of a small cubic term, lend-

ing further support for the theory of HLM. This comparison also shows that the dynamics of interfaces are especially sensitive for the N -Sm- A transition because these materials are transparent to light so that the interface may be directly observed.

III. LANDAU DESCRIPTION OF PHASE TRANSITIONS WITH A CUBIC TERM

To reveal universal features of data taken under widely different conditions, the relation between all the measured parameters must be derived. In this section, we will therefore derive a number of scaling expressions for the free energy (4) in the mean-field approximation.

When $B = 0$ in Eq. (4), $C < 0$ describes first order phase transitions and $C > 0$ second-order phase transitions. If $B \neq 0$, the transition remains first order even for $C > 0$: as the transition temperature is approached from above, the coherence length remains finite and from below, the order parameter is nonzero. We refer to the condition $C = 0$ as the Landau tricritical point even when $B \neq 0$. In this analysis, we exploit the finiteness of the parameters of the phase transition at the LTP to scale all quantities by values assumed at this point. A relatively simple universal function results that depends only on the identification of the LTP.

A. Relationship between the susceptibility, coherence lengths, and latent heats

The scaling expressions derived in this section follow directly from the free energy (4) in the mean-field approximation. Readers not interested in the derivation can skip to the main results, Eqs. (18)–(20).

On a first-order transition line, the order parameter ψ jumps discontinuously from $\psi = 0$ to ψ_c at $T_{N\text{-Sm-}A}$. In the following, we take $\psi > 0$ and do not carry the absolute value sign in the cubic term. Since we do not consider fluctuations and because of the even symmetry of Eq. (4) guaranteed by the absolute value sign, limiting ourselves to this case does not detract from the generality of this procedure. In the mean-field approximation, then, ψ_c can be determined by minimization of Eq. (4) and requiring that the free energies of the ordered (A phase, $\psi \neq 0$) and the disordered (N phase, $\psi = 0$) phases are equal. This yields

$$\frac{2}{\psi_c^2} f = A_c - \frac{2}{3} B \psi_c + \frac{1}{2} C \psi_c^2 + \frac{1}{3} E \psi_c^4 = 0 \quad (\psi_c > 0), \quad (6)$$

and

$$\frac{1}{\psi_c} \frac{df}{d\psi} = A_c - B \psi_c + C \psi_c^2 + E \psi_c^3 = 0 \quad (\psi_c > 0). \quad (7)$$

The phase transition line is found by subtracting these two equations to obtain

$$B - \frac{3}{2} C \psi_c - 2 E \psi_c^3 = 0 \quad (\psi_c > 0). \quad (8)$$

ψ_c is then the single positive root of Eq. (8). We assume E and B are positive constants that do not vary for a homologous series of compounds (compounds that differ

only in the length of their aliphatic chains), and that A goes linearly through zero at a temperature T_0 ($\neq T_{N-Sm-A}$), so that $A = a'\epsilon$ with $\epsilon \equiv (T - T_0)/T_0$.

At the LTP, $C = 0$ so that

$$\psi_c^* = \left[\frac{B}{2E} \right]^{1/3}. \quad (9)$$

Substitution of this result in Eq. (6) shows that the various coefficients at the LTP are related by

$$A_c^* = a'\epsilon_c^* = E \left[\frac{B}{2E} \right]^{4/3} = E(\psi_c^*)^4 = \frac{B}{2}\psi_c^*. \quad (10)$$

Throughout this paper, an asterisk will be used to denote values assumed at the LTP. Substituting the results of Eqs. (9) and (10) into Eq. (7), we obtain

$$\frac{A_c}{A_c^*} = 2 \frac{\psi_c}{\psi_c^*} - \frac{C}{A_c^*} \psi_c^2 - \left[\frac{\psi_c}{\psi_c^*} \right]^4. \quad (11)$$

Equation (8) relates the coefficient C to the distance from the LTP as

$$\frac{3}{4} \frac{C}{E} = -(\psi_c^*)^2 \left[\left[\frac{\psi_c}{\psi_c^*} \right]^2 - \frac{\psi_c^*}{\psi_c} \right], \quad (12)$$

or, with the aid of Eq. (10),

$$\frac{C}{A_c^*} = -\frac{4}{3} \frac{1}{(\psi_c^*)^2} \left[\left[\frac{\psi_c}{\psi_c^*} \right]^2 - \frac{\psi_c^*}{\psi_c} \right]. \quad (13)$$

With this expression, we may further simplify Eq. (11) to

$$\frac{A_c}{A_c^*} = \frac{2}{3} \frac{\psi_c}{\psi_c^*} + \frac{1}{3} \left[\frac{\psi_c}{\psi_c^*} \right]^4. \quad (14)$$

Since the latent heat is related to the jump in the entropy by $L = \Delta S/R$, we obtain in the mean-field approximation

$$\frac{\Delta S}{R} = \frac{L}{RT_{N-Sm-A}} = \frac{\partial f}{\partial \epsilon} = \frac{1}{2} a' \psi_c^2, \quad (15)$$

so that together with (9),

$$\frac{\Delta S^*}{R} = \frac{1}{2} a' \left[\frac{B}{2E} \right]^{2/3}. \quad (16)$$

The inverse susceptibility χ_c^{-1} in the disordered phase on the transition line is

$$\chi_c^{-1} = \left. \frac{\partial^2 f}{\partial \psi^2} \right|_{\psi=0} = A_c. \quad (17)$$

Thus, in the mean-field limit, using the definitions in Eqs. (15)–(17), Eq. (14) can be related to the entropy jump at the transition by the universal scaled relationship:

$$\frac{\chi_c^*}{\chi_c} = \frac{A_c}{A_c^*} = \left[\frac{\Delta S}{\Delta S^*} \right]^2 \left[\frac{1}{3} + \frac{2}{3} \left[\frac{\Delta S}{\Delta S^*} \right]^{-3/2} \right]. \quad (18)$$

Equation (18) is a simple way to relate the measured latent heat ($L = T_{N-Sm-A} \Delta S$) to the susceptibility that in turn can be related to the relevant parameters of the tran-

sition by scaling. For example, the coherence length measured at T_{N-Sm-A} in mean field is $\xi_c^2 \sim \chi_c$ so that

$$\frac{\xi_c^*}{\xi_c} = \left[\frac{A_c}{A_c^*} \right]^{1/2} = \left[\frac{\Delta S}{\Delta S^*} \right] \left[\frac{1}{3} + \frac{2}{3} \left[\frac{\Delta S}{\Delta S^*} \right]^{-3/2} \right]^{1/2}. \quad (19)$$

Equations (18) and (19) are particularly useful as they only depend implicitly on the location of the LTP.

When $\Delta S/\Delta S^* \gg 1$, for negative values of C , $A_c/A_c^* \approx \frac{1}{3}(\Delta S/\Delta S^*)^2$ and $A_c \approx \frac{3}{16} C^2/E$, a classical result for the case in which a line of first-order transitions ($B=0, C<0$) ends at LTP and becomes a line of second-order phase transitions for $C>0$. When $\Delta S/\Delta S^* \ll 1$, $A_c/A_c^* \approx \frac{2}{3}(\Delta S/\Delta S^*)^{1/2}$ and $A_c \approx \frac{2}{9} B^2/C$, also a well known result for the case in which $B \neq 0, E=0$. Thus, as $B \rightarrow 0$, $A_c \rightarrow 0$ like B^2 and $\xi_c \rightarrow \infty$ like $1/B$.

B. Dependence of C on concentration in mixtures

McMillan⁴ and de Gennes⁵ predicted that molecular length would be an important parameter to drive the N - $Sm-A$ transition towards an LTP. In this theory, the shorter the molecular species exhibiting an N - $Sm-A$ transition, the less likely they were to exhibit the smectic- A phase, therefore the larger the temperature range of the nematic phase and the more likely the transition was to be second order. Thus, adding similar but longer molecular species in a concentration x would tend to drive C to zero like $C = C_0(x - x^*)$, with $C_0 < 0$, because of the coupling between orientational and translational order (as before, x^* is the value of the concentration at the LTP). This behavior of C is in agreement with the analytical form predicted by Landau.

Substituting the linear dependence of C on x into Eq. (13), a universal function of the distance to the LTP can be found as

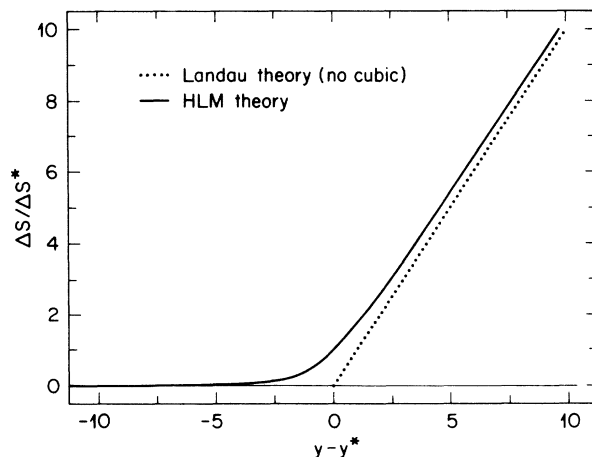


FIG. 1. Universal crossover behavior for $\Delta S/\Delta S^*$ as a function of the concentration variable $y - y^*$ near the LTP, as given by Eq. (20).

$$\left[\frac{\Delta S}{\Delta S^*} \right] - \left[\frac{\Delta S}{\Delta S^*} \right]^{-1/2} = \frac{\alpha R}{\Delta S^*} (x - x^*) \equiv y - y^*, \quad (20)$$

where $\alpha = -\frac{3}{8}(a'C_0/E)$. When $\Delta S/\Delta S^* \gg 1$, one obtains the classical result of Landau theory: $y - y^* = \Delta S/\Delta S^*$ and $\Delta S/R = \alpha(x - x^*)$ valid far from the LTP or everywhere if $B = 0$. When $\Delta S/\Delta S^* \ll 1$, C is large and positive thus $y - y^* = -(\Delta S/\Delta S^*)^{1/2}$ and $\Delta S/R = \frac{2}{9}[a'B^2/C_0^2(x - x^*)^2]$. The universal crossover function Eq. (20) is shown in Fig. 1. Far from the LTP, assuming $a' \approx 1$, $C \approx 1$, and $B \approx 10^{-2}$, one has $\Delta S/R \approx 10^{-5}$. This value is not measurable even by the finest adiabatic calorimeter. However, near the LTP the situation is different. According to Eq. (16), $\Delta S^*/R \approx 10^{-2} - 10^{-1}$ (again taking $a' \approx E \approx 1$ and $B \approx 10^{-2}$) i.e., quite accessible to adiabatic scanning calorimetry. Next, we investigate the latent data for three mixtures using the results from this section.

IV. COMPARISON OF CALORIMETRIC MEASUREMENTS WITH MEAN-FIELD SCALING

A. Phase diagrams of $\bar{6}O10$ - $\bar{6}O12$ and n CB mixtures

In Ref. 7, the results of the adiabatic scanning calorimetry measurements of the N -Sm- A latent heat in $\bar{6}O10$ (4- n -hexyloxy-phenyl-4'- n -decyloxybenzoate)- $\bar{6}O12$ (4- n -hexyloxyphenyl-4'- n -dodecyl-oxybenzoate) mixtures were reported. The smectics- A formed by molecules of this series are usually the one layer phases. The only peculiarity of the phase diagram of this mixture is that the nematic-smectic- A -isotropic triple point coincides with pure $\bar{6}O12$ (Fig. 2). Far from the apparent tricritical point the concentration dependence of the latent heat is close to linear, but when the latent heats become small, they deviate from this linear behavior (Fig. 3). The latent heat becomes too small to measure in this data set at the apparent tricritical point at $x \approx 0.4$.

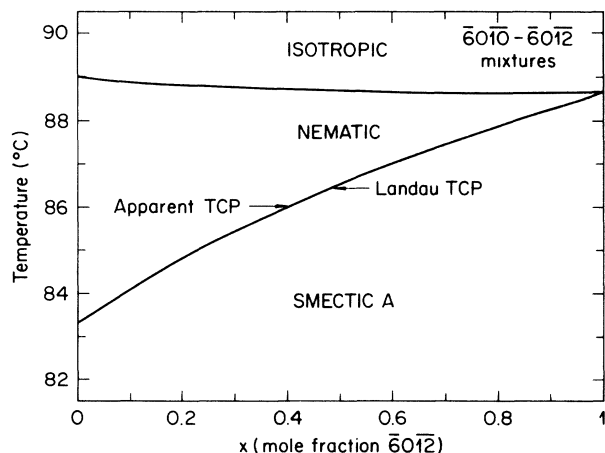


FIG. 2. Phase diagram of the $\bar{6}O10$ - $\bar{6}O12$ mixtures. The arrow labeled "Apparent TCP" indicates the point at which the latent heat becomes immeasurably small, the one labeled "Landau TCP" the tricritical point as determined from the fit to the crossover function with a cubic term included, shown in Fig. 3.

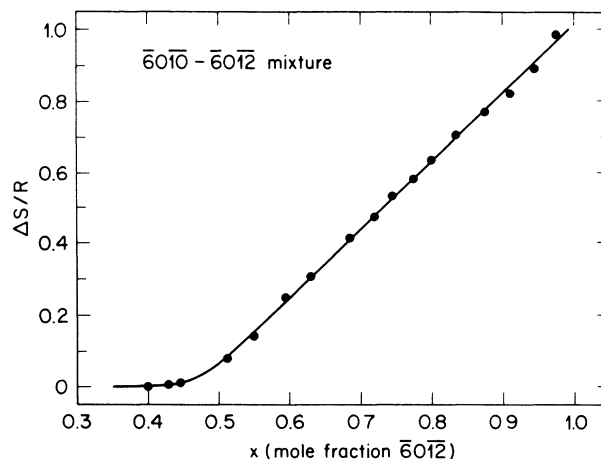


FIG. 3. The latent heat of the $\bar{6}O10$ - $\bar{6}O12$ mixture fit to the crossover form Eq. (20).

Another system which was studied is the n CB (where CB represents cyanobiphenyl) compounds, since coherence length, latent heat, and velocity measurements have been made for the pure materials 8CB and 9CB as well as several mixtures of 9CB and 10CB. The n in n CB refers to the length of the aliphatic chains associated with these molecules. Thus, 8CB is shorter than 9CB which in turn is shorter than 10CB. A layer thickness intermediate between that of the pure materials is observed in the smectic phase of binary mixtures.

In agreement with McMillan's ideas,⁴ 8CB, being the shortest molecule, exhibits a N -Sm- A transition that appears truly second order on the basis of adiabatic scanning calorimetry and x-ray measurements. With increasing concentration of 10CB, the temperature range of the nematic phase narrows linearly and disappears at $x \approx 65\%$ 10CB in 8CB (Fig. 4). Concentrations richer in 10CB transform directly from the smectic- A phase to the isotropic liquid state. Adiabatic scanning calorimetry identifies an apparent tricritical point at $\sim 30\%$ 10CB in 8CB where the latent heat becomes immeasurably small¹² (see Fig. 5). The x-ray data are not available for these mixtures but have been published for 9CB, 10CB, and their binary mixtures. Therefore, we also studied these compounds.

For the 9CB-10CB studies, x-ray measurements⁹ reported a tricritical point at $\sim 10\%$ 10CB in 9CB; i.e., 9CB appeared second order. Latent heat measurements,⁶ however, find that 9CB is weakly first order. (See Fig. 6.) From these measurements, there is thus some doubt about the order of the N -Sm- A phase transition of 9CB, but as we shall see, the dynamical measurements find that all the compounds, including 8CB and 9CB, exhibit front dynamics consistent with a first-order N -Sm- A transition.¹⁴

B. Crossover behavior of the latent heat at the N -Sm- A transition of mixtures

Accurate measurements of the latent heat on the N -Sm- A transition line were carried out by Marynissen

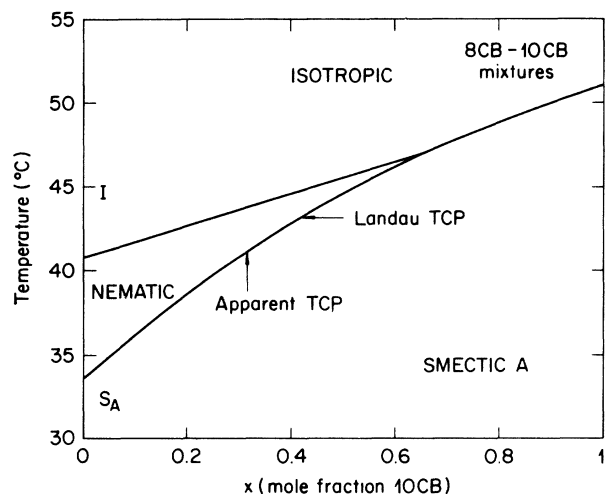


FIG. 4. Phase diagram of the 8CB-10CB mixtures, after Ref. 12.

*et al.*⁶ on the 8CB-10CB and 9CB-10CB mixtures using high resolution adiabatic scanning calorimetry (Figs. 5 and 6). They described the decrease in latent heat they observed in these mixtures by a quadratic dependence of L on the concentration difference $L \sim (x - x_i)^2$ for x near x_i , where x_i is the concentration of the apparent tricritical point. As argued first in Ref. 18, we believe that the nonlinear relation they observed between L and x is a consequence of a cubic term in the Landau free energy [Eq. (4)] that becomes evident near a Landau tricritical point.

In the n CB mixtures the LTP is too close to the nematic to isotropic transition to clearly observe the linear concentration dependence of ΔS seen far from the LTP in the $\bar{6}O10$ - $\bar{6}O12$ mixtures—compare Fig. 3 with Figs. 5 and 6. We fitted all calorimetric data with formula (20); Figs. 7 and 8 show all the data plotted in the universal

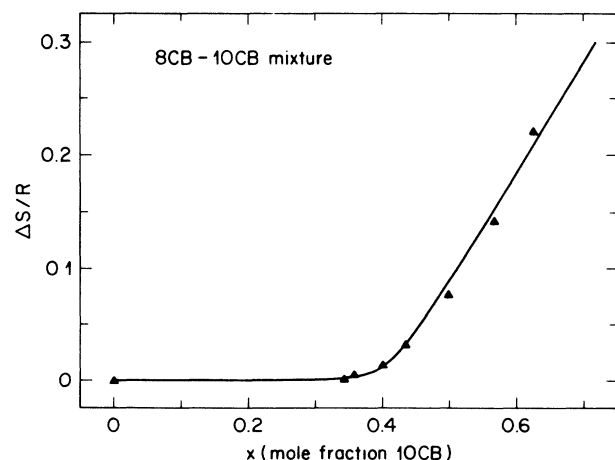


FIG. 5. Latent heat data from Ref. 12 for the 8CB-10CB mixtures fitted to the scaling function (20) to determine x^* and ΔS^* . The data point for the pure 8CB was not included in the fit.

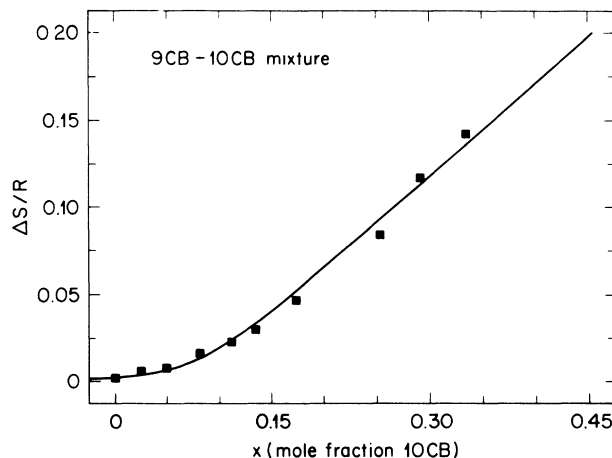


FIG. 6. Latent heat data from Ref. 12 of the 9CB-10CB mixtures fitted to the scaling function (20) to determine x^* and ΔS^* .

normalized form. Upper limits are shown for the latent heats that have not been included in the fit. The results of the fits are summarized in Table I.

Since Eq. (20) provides a good, quantitative description of the data even when mixtures that do not exhibit an observable latent heat are included in the fitting procedure, we conclude that Figs. 7 and 8 show that the experimental evidence is quite consistent with the existence of the cubic term to describe this transition as predicted by the HLM theory. Additional support for the theory for mixtures (and pure compounds) that have immeasurably small latent heats are provided by the new dynamic technique¹⁴ that we discuss next.

V. DYNAMIC TECHNIQUE FOR ASSESSING PHASE TRANSITION ORDER

The dynamic behavior of interfaces does not directly detect discontinuities in the thermodynamic properties

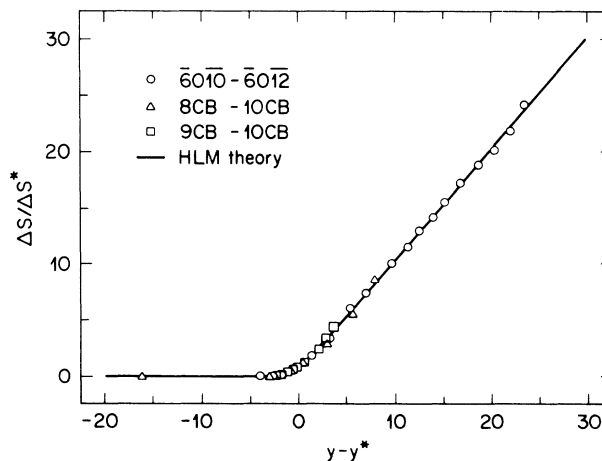


FIG. 7. Normalized universal form showing that Eq. (20) describes the 8CB-10CB, 9CB-10CB, and $\bar{6}O10$ - $\bar{6}O12$ mixtures.

TABLE I. Parameters obtained from fitting the latent heat data (Refs. 6 and 12) Eq. (20) and used in fitting the velocity data (Ref. 14) to Eqs. (28) and (29).

Mixture	x^*	$\Delta S^*/R$	α	$(v/\epsilon')^*$ (cm/sec)
9CB-10CB	0.0983	0.0192	0.518	770
8CB-10CB	0.4243	0.0261	0.993	540
6O10-6O12	0.4828	0.0408	1.947	

but reflects the form of the free-energy potential driving the interface motion. Cladis *et al.*¹⁴ were the first to realize that this *qualitative* difference in the dynamic behavior of interfaces can already be a powerful tool for determining the order of a phase transition when the interface can be directly observed, and they used it to study the N -Sm- A transition. In the following, we first describe the basic idea underlying their approach, and then show that, in combination with the analysis of the preceding sections, even *quantitative* comparisons can be made.

A. General description of dynamics of propagating interfaces

Let us first compare the possibility of creating fronts and interfaces near a second order and a first order phase transition before analyzing the dynamics in detail. For simplicity, we will present the discussion directly in the language of the mean-field approximation relevant to the N -Sm- A transition, but most observations apply also to the more general case in which critical fluctuations are important. Also, we will assume that the temperature is homogeneous throughout the sample, in other words, we assume that no temperature gradients are externally imposed and that the latent heat is negligible. We will come back to these effects later.

In Figs. 9(a) and 9(b) we illustrate the form of the local free energy density $f(\psi)$ for the case of a *first-order transition*. Above T_c [Fig. 9(a)], the absolute minimum of $f(\psi)$ corresponds to the disordered state $\psi=0$, while below T_c [Fig. 9(b)], the free energy density has its abso-

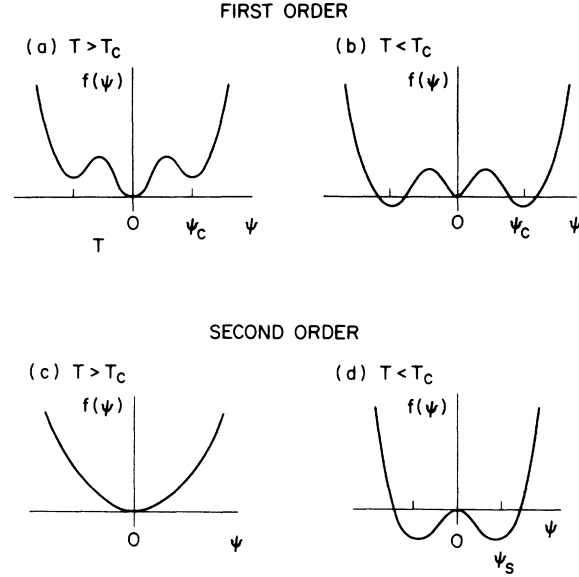


FIG. 9. Illustration of the form of the free-energy $f(\psi)$ for first- and second-order transitions.

lute minimum at $\psi \neq 0$. However, even when $T < T_c$, the disordered state $\psi=0$ still corresponds to a local minimum, so it is only metastable. As a result, there is a finite surface free energy between the two states and a nucleation barrier for the ordered state to form. Thus, as is well known, the disordered state can be undercooled, i.e., can be brought to a temperature $T < T_c$; likewise, the ordered state can be overheated. A related manifestation of the existence of the barrier in $f(\psi)$ between the two minima is the fact that by increasing or decreasing the temperature around T_c , interfaces at a first-order transition can be made to propagate in either direction, corresponding to melting or freezing of the ordered state. Moreover, if the interface is rough, the interface velocity is linear in $\Delta T = T - T_c$, so that the response is symmetric about T_c . Within the Ginsburg-Landau approach, this result can be obtained as follows.

Consider for simplicity an isotropic free energy

$$F = \int d\mathbf{r} \left[\frac{1}{2M} (\nabla\psi)^2 - f(\psi) \right], \quad (21)$$

whose dynamics are governed by the time-dependent Ginsburg-Landau equation

$$\tau_0 \frac{\partial \psi}{\partial t} = - \frac{\delta F}{\delta \psi} = \frac{1}{M} \nabla^2 \psi - \frac{df}{d\psi}. \quad (22)$$

Here τ_0 is the microscopic (bare) relaxation time of the smectic order parameter. For a profile $\psi_0(x - vt)$ propagating with a constant speed v between the state $\psi = \psi_1$ on the left ($x \rightarrow -\infty$) and $\psi = \psi_2$ on the right ($x \rightarrow \infty$), we have

$$-v\tau_0 \frac{d\psi_0}{dx} = \frac{1}{M} \frac{d^2\psi_0}{dx^2} - \frac{df(\psi)}{d\psi}. \quad (23)$$

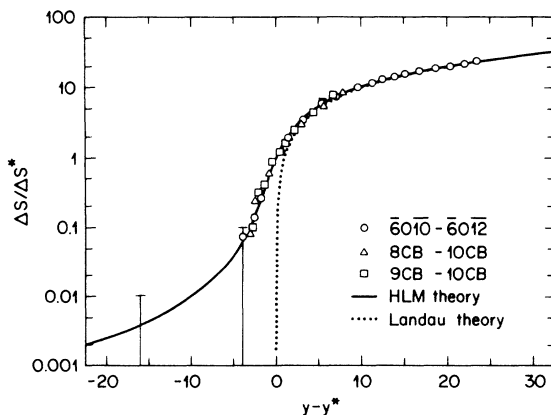


FIG. 8. Normalized universal scaling form on a log scale for the latent heat.

Upon multiplying this equation by $-d\psi_0/dx$ and integrating, we see that the gradient terms drop out to yield

$$\begin{aligned} \tau_0 v \int_{-\infty}^{+\infty} dx \left[\frac{d\psi_0}{dx} \right]^2 \\ = \int_{-\infty}^{+\infty} dx \left[-\frac{1}{2M} \frac{d}{dx} \left[\frac{d\psi_0}{dx} \right]^2 + \frac{d\psi_0}{dx} \frac{df}{d\psi} \right] = \Delta f, \end{aligned} \quad (24)$$

where $\Delta f = f_2 - f_1$ is the difference between the free-energy densities of the two states. Since near a first-order transition Δf is linear in $T - T_c$, and since the integral on the left is positive for all T near T_c [$d\psi_0/dx$ in the integral can be approximated, to lowest order, by the $v=0$ solution of Eq. (23)], this equation confirms that the region corresponding to the lowest free-energy state expands. Moreover, in view of the fact that Δf is linear in $\Delta T \equiv T - T_c$, it confirms that v goes linearly through zero at T_c : $v \propto \Delta T$. We will explore Eq. (24) in more detail later.

Near a second-order phase transition, on the other hand, the behavior is very different. In this case, one normally does not see well-defined interfaces. To understand the reason within a mean-field picture, consider Figs. 9(c) and 9(d), where we have sketched the form of f near a second-order transition. Above T_c , $f(\psi)$ has just a single minimum at $\psi=0$; for $T < T_c$, however, $f(\psi)$ has a local maximum at $\psi=0$ and an absolute minimum at some finite value(s) $\psi \neq 0$. If we imagine a situation in which a system, initially at $T < T_c$ (so $\psi \neq 0$) is suddenly brought to a temperature $T > T_c$, ψ will relax essentially *homogeneously* to zero since as illustrated in Fig. 9(c), $df/d\psi \neq 0$ for all $\psi \neq 0$. Thus, in contrast to the behavior at a first-order transition, *no* propagating interfaces can be created by suddenly increasing the temperature above a second-order transition temperature T_c . For quenches from $T > T_c$ to $T < T_c$, the situation is different, however. In this case, the driving force in the bulk, where $\psi=0$, vanishes since $df/d\psi=0$. If fluctuations and initial inhomogeneities would be sufficiently small, one could therefore in principle enter a regime in which the dynamics are dominated by interfacelike fronts that propagate into the *unstable* state $\psi=0$. A simple scaling analysis shows that the speed of such fronts should vary as $v \propto \sqrt{|T - T_c|}$ (the proportionality factor is known from various theoretical approaches²¹). Of course, the creation of such a front would not be feasible at phase transitions in liquid crystals, where fluctuations are large. In this case, one would expect to see a rapid local growth of smectic patches everywhere in the sample rather than the creation of well-defined fronts. Nevertheless this type of front propagation into unstable states has successfully been studied near the Rayleigh-Bénard and Taylor-Couette instabilities^{22,23} where inhomogeneities and fluctuations can be suppressed sufficiently. The speeds of such fronts were found to agree with the above-mentioned scaling.²⁴

In summary, propagating interfaces naturally occur upon quenching or overheating a system that exhibits a

first-order phase transition, and the dynamics are symmetric and linear about T_c . Near a second-order transition, however, fronts can only be created under carefully controlled experimental conditions and their dynamics are very asymmetric: on one side of T_c well-developed fronts do not exist, while on the other side of T_c , their velocity increases as $\sqrt{|\Delta T|}$.

B. Scaling relations near weakly first-order transitions

Let us now return to the case of a moving interface near a first-order transition and investigate the scaling behavior implied by Eq. (24). From Eq. (15), we see that one has $f_2 - f_1 = \frac{1}{2} a' \psi_c^2 \epsilon'$ ($\epsilon' \equiv (T - T_c)/T_c$ is the dimensionless distance from the first-order transition temperature T_c). Since the integral in (24) will scale as ψ_c^2/ξ_c , we obtain for the slope v/ϵ' the scaling result

$$\frac{v}{\epsilon'} \propto \frac{a' \xi_c}{\tau_0}. \quad (25)$$

According to this expression, the interface moves faster the larger ξ_c is. Physically, this reflects the fact that the friction experienced by a moving interface is smaller the smaller ψ_c is and the larger the interface width is (since $\partial\psi/\partial t = -v\partial\psi/\partial x$ is smaller). As described below, the slope v/ϵ' can be obtained from the dynamical measurements of Cladis *et al.*¹⁴ In combination with the scaling result (19) for ξ_c , the velocity measurements can then be compared with those of the correlation length ξ_c as well as the latent heat measurements by writing Eq. (25) in the form

$$\frac{v/\epsilon'}{(v/\epsilon')^*} = \frac{\xi_c}{\xi_c^*}. \quad (26)$$

In writing this scaling relation, we have assumed that the microscopic time τ_0 and the parameter a' do not vary appreciably from mixture to mixture. Moreover, we neglect the variation of the prefactor in (25) that depends on the relative size of the coefficients B , C , and E and hence on the composition of the mixture. This last effect can actually be accounted for. From the Ginsburg-Landau equation (22) with f of the form (4), it is easy to show that in general one has near the first-order transition

$$\frac{v}{\epsilon'} = \frac{a' \xi_c}{\tau_0} g \left[\frac{C}{B^{2/3} E^{1/3}} \right] (\epsilon' \rightarrow 0), \quad (27)$$

where $\xi_c \equiv (a' \epsilon_c M)^{-1/2}$ is the correlation length at T_c on the *disordered* (nematic) side of the transition. From the solutions of the interface propagation problems for $B=0$, $C<0$, $E>0$ and for $E=0$, $B>0$, $C>0$, it follows that²⁵ $g(-\infty)=2$ and that²⁶ $g(+\infty)=3$. For $B \neq 0$, we have obtained g numerically from dynamical simulations of the Ginsburg-Landau equation. As Fig. 10 shows, the factor g varies monotonically between these two values, the variation being such that in the scaling relation (26), v tends to be underestimated on the “second-order side” $C<0$ and overestimated on the “first-order side” $C>0$ of the LTP. Nevertheless, since g varies only about $\pm 20\%$ with respect to its value at the LTP, we will

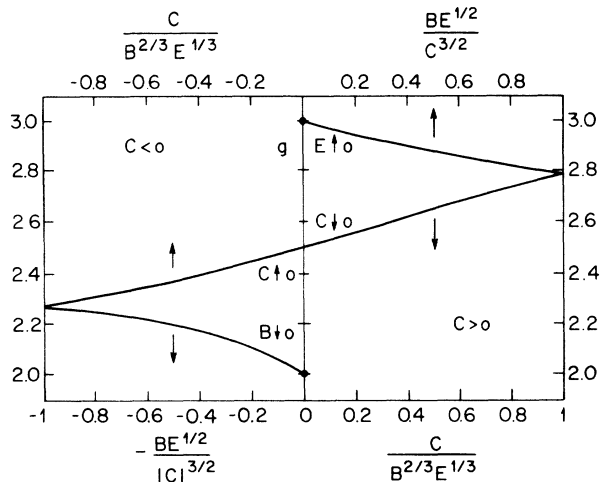


FIG. 10. The factor g defined in Eq. (27) as a function of $C/B^{2/3}E^{1/3}$, as obtained from the numerical solution of the Ginzburg-Landau equation.

henceforth neglect this effect and use Eq. (26) to compare the experimental data.

In the above discussion, we have assumed that the temperature of the sample remains homogeneous. However, at a first-order transition, the latent heat will induce a temperature jump across the interface of order L/c , where c is the heat capacity, so the above picture is only accurate if L is small enough that this temperature difference is small compared to the difference from T_c , ΔT , or if the cell geometry is such that the heat is conducted away sufficiently fast. If these conditions are not met, the interface dynamics are not intrinsic anymore, but instead become diffusion limited. Likewise, in practice care must be taken to ensure that the temperature of the experimental cell is sufficiently homogeneous, since in the presence of a temperature gradient an apparent interface can be created even at a second-order transition. Upon changing the temperature of the cell, the dynamics of such gradient-induced interfaces will generally follow the temperature response of the cell, as the position of the interface will “ride” on the $T = T_c$ isotherm.

VI. RESULTS OF DYNAMICAL MEASUREMENTS ON 8CB-10CB AND 9CB-10CB MIXTURES

As described in Ref. 14, dynamical measurements of the type discussed above were done on a large number of mixtures. In this section, we first briefly describe the experimental procedure, and then analyze the data for the 8CB-10CB and 9CB-10CB mixture in terms of the scaling expression discussed above.

A. Description of the experiments

The experiments were performed on glass and sapphire cells that were typically $13\ \mu\text{m}$ thick; a region of about $1\ \text{mm}$ of the cell could be viewed through a microscope with a video camera. The procedure was to start at a uniform temperature within 0.02°C of T_c , rapidly change the temperature to some value T on the other side of T_c ,

wait typically a few seconds for the front to appear in the field of view, and then record the front passage with a video monitor. From a frame-by-frame analysis, the speed $v(\epsilon)$ was found, with a resolution $0.1\ \text{s}$. In all the experiments, stationary as well as moving interfaces were observed—as discussed above, a signature that the N - Sm-A transition in all the samples studied was weakly first order. The data for v as a function of temperature for the 8CB-10CB mixtures can be found in Ref. 14, while we present the experimental results for pure 9CB and for 22.4% 10CB in 9CB in Fig. 11. For the 22.4 mol. % mixture, the front velocity clearly goes linearly through zero as expected for weakly first-order transitions with a small but measurable latent heat (the LTP is estimated to be at $x^* \approx 9.8\%$; see also Fig. 6). Although the uncertainty in temperature is the same for the 9CB as for the mixture, its steepness precludes a precise determination of the slope as for the 22.4% mixture. Nevertheless, these data are consistent with a linear dependence of v on ϵ' . The data for some ten other compositions¹⁴ between these two values fall between these two extremes.

As discussed, temperature gradients can induce an apparent interface; however, as the following observations suggest, it is unlikely that the interfaces seen experimentally were due to such gradients. (i) Small ($2 \times 2.5 \times 0.7\ \text{mm}^3$) platinum resistance thermometers, thermally sunk to the cells, measured the temperature accurately to 0.01°C . The data used in the analysis were all taken at constant temperature. (ii) Cells made of two glass plates $1\ \text{mm}$ thick or two sapphire plates $0.5\ \text{mm}$ thick with the liquid crystal in the $13\text{-}\mu\text{m}$ gap between the plates were used. Although the thermal diffusivity of sapphire is 26 times larger than the one of glass, within the experimen-

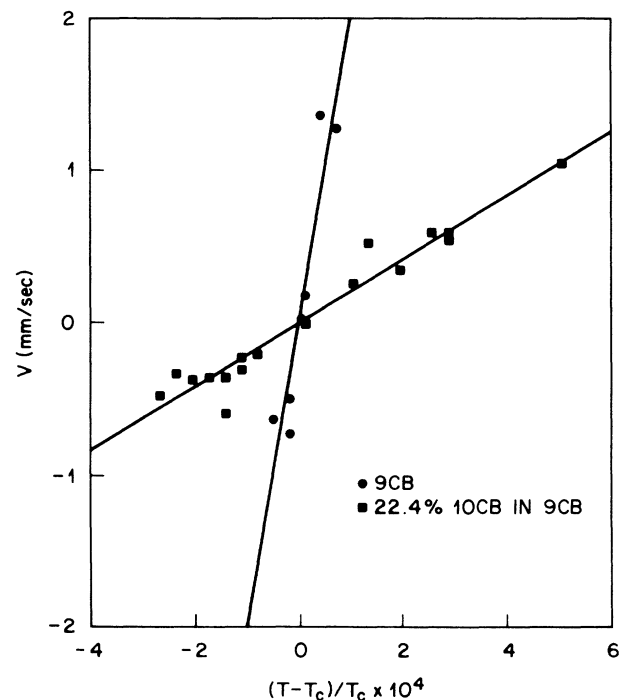


FIG. 11. Interface velocity v vs $\epsilon' = (T - T_c)/T_c$ for pure 9CB and the 22.4% 10CB in 9CB mixture.

tal accuracy of 20%, the interface velocities were found to be the same in both cells. Thus it was concluded that interface motion was not driven by thermal relaxation of the cell and not governed by heat release in the interfacial region. (iii) The data did not show a detectable asymmetry for cooling or heating. (iv) The field of view was always at a fixed position with respect to the heaters. With a given part of the cell in the field of view, the interface was found to propagate in a fixed direction with respect to the sample, presumably determined by a nucleation site. When a different part of the cell was brought in the field of view, the propagation direction was different with respect to the heaters. It was therefore concluded to be unlikely that systematic temperature gradients played a role. (v) In a narrow range around T_c , static interfaces were observed; these were pinned at certain spots of the cell that presumably are imperfections. Pinning is associated with the existence of a surface tension, and hence is a feature of a first-order transition (no surface tension can be associated with a front between a stable and unstable state).

B. Analysis of velocity and coherence length data

Figures 12 and 13 show a plot of the slope v/ϵ' as a function of concentration for the 8CB-10CB and 9CB-10CB mixtures. In Ref. 14, the velocity data were compared directly with estimates of the correlation length ξ_c . However, since ΔS is measured more accurately, we have here chosen to fit the data by eliminating ξ_c in favor of ΔS using Eqs. (19) and (20). In this way, the solid lines in Figs. 12 and 13 give the velocity of each series of mix-

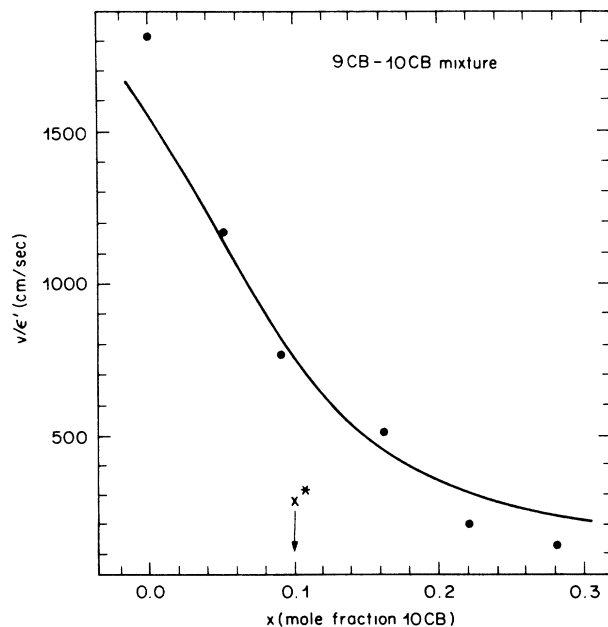


FIG. 12. Front speed plotted against concentration for the 9CB-10CB mixtures. The solid line is based on Eqs. (19), (20), and (26) and the fit for the 9CB-10CB mixture in Fig. 6.

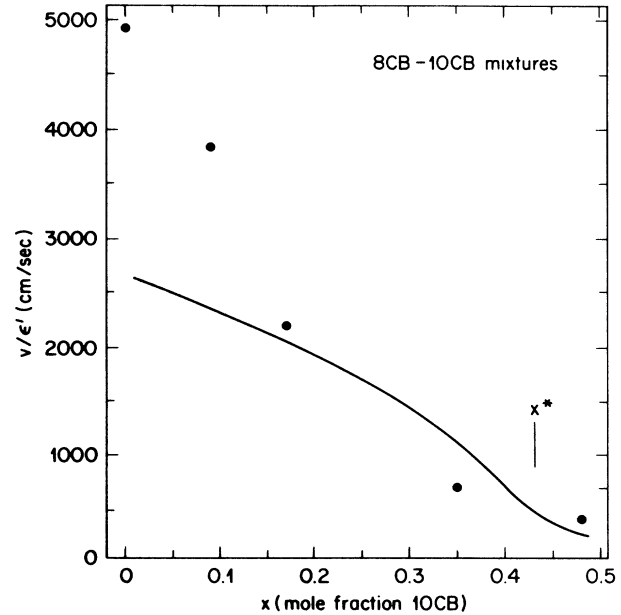


FIG. 13. Front speed plotted against concentration for the 8CB-10CB mixtures. The solid line is based on Eqs. (19), (20), and (26) and the fit for the 8CB-10CB mixtures in Fig. 5.

tures as an implicit function of the concentration x according to

$$\frac{v}{\epsilon'} = \left[\frac{v}{\epsilon'} \right]^* s^{-1} \left(\frac{1}{3} + \frac{2}{3}s^{3/2} \right)^{-1/2}, \quad (28)$$

$$x = \frac{bx^* + s - s^{-1/2}}{b}, \quad (29)$$

where $s \equiv \Delta S / \Delta S^*$ and $b = \alpha R / \Delta S^*$. The values of b and x^* are taken from Table I and so are based on the fit to the latent heat data. The agreement for the 9CB-10CB mixtures is remarkable, taking into account that the solid curve is obtained without adjustable parameters other than the slope $(v/\epsilon')^*$ at the LTP, whose value is also given in Table I. For the 8CB-10CB mixture, on the other hand, the agreement is only qualitative; however, the last two points are far away from the LTP where the experimental error bars are large (in Ref. 14, the error was estimated to be 50% for the 8CB data point) and where we have no reason to expect the mean-field approximation to stay accurate. Note also that if we would take into account the variation of the factor g in Eq. (26), this would move the solid line upward (the velocities for small concentrations would become larger), and so it would bring the predicted values a little closer to the data points.

We now wish to compare the various data with those for the coherence length ξ_c . Accurate x-ray measurements of ξ_c have been performed by Ocko, Birgeneau, and Litster⁹ on the mixtures we consider. However, the comparison of the experimental results is complicated by the fact that even near the LTP, there is considerable anisotropy in ξ_c measured in the nematic phase. Correla-

tion lengths parallel and perpendicular to \mathbf{n} diverge with different effective exponents (ν_{\parallel} and ν_{\perp} , respectively) that depend on the temperature range of the nematic phase. In mean-field approximation, one expects near the LTP that $\nu_{\parallel} = \nu_{\perp} = \frac{1}{2}$, but the x-ray data do not support this. (Possibly, one observes a crossover due to the enhanced Fisher renormalization near the LTP.¹⁹) Moreover, only three mixtures (14%, 20%, and 28% 10CB in 9CB) were observed to show evidence of a finite ξ_c at the first-order transition temperature, so for most mixtures the x-ray scattering data only give a lower bound for ξ_c .

If, in spite of these caveats, the slope ν/ϵ' is plotted versus the average correlation length $\xi_c = (\xi_{\parallel}^2 \xi_{\perp})^{1/3}$ as done in Fig. 1 of Ref. 14, the data are reasonably consistent with the scaling relation (27). With $a'g = 1$, a microscopic relation time τ_0 of about 7.5×10^{-9} s was obtained from this plot. Since diffusion coefficients are typically of the order of 4×10^{-7} cm²/s, this value is consistent with the naive expectation that τ_0 should be of order of the time it takes a molecule to diffuse half a layer spacing.

In Fig. 14, we compare the measurements obtained by different methods. Along the horizontal axis, we plot $\Delta S/\Delta S^*$ as determined from the (fit to the) calorimetric data, and along the vertical axis the ratio $(A^*/A)^{1/2}$. Since in a mean-field approximation this ratio equals ξ_c/ξ_c^* , this quantity can be used to plot both the data for the correlation length (triangles) from x-ray experiments and the data for the interface response ν/ϵ' (dots for the 9CB-10CB mixtures, crosses for the 8CB-10CB mixtures). The triangles denote the values of the correlation lengths in 9CB-10CB mixtures as measured by Ocko, Birgeneau, and Litster;⁹ a triangle with a horizontal bar denotes the

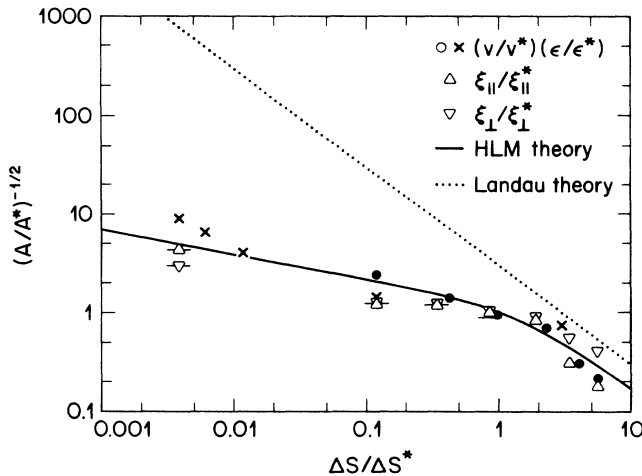


FIG. 14. Comparison of the data from three different experiments. The ratio $(A^*/A)^{1/2}$ plotted along the vertical axis is equal to ξ_c/ξ_c^* . The solid dots denote data points from the dynamical measurements in the 9CB-10CB mixtures, the crosses those for the 8CB-10CB mixtures. Triangles denote correlation lengths measured by Ocko, Birgeneau, and Litster (Ref. 9). A triangle with a horizontal bar indicates a lower bound to the correlation length, as the transition was concluded to be second order on the basis of the x-ray measurements.

largest correlation length measured at compositions that were concluded to have a second-order phase transition. Hence the data points with a horizontal bar are a *lower-bound* only to ξ_c/ξ_c^* . The solid line in this figure is the mean-field scaling function which is given by (19) without adjustable parameters. Although the fit is not perfect, we conclude that all data points are consistent with the trend given by (19), a crossover from $\xi_c \propto (\Delta S)^{-1}$ to $\xi_c \propto (\Delta S)^{-1/4}$. Since in the absence of the cubic term $-B|\psi|^3$ in the free energy predicted by HLM the data should follow the scaling $\xi_c \propto (\Delta S)^{-1}$ throughout the first-order region (so that they would lie parallel to the dotted line in the figure), we conclude that the crossover manifest in the data points from three different types of experiments provide good evidence for the HLM effect at the N -Sm- A transition near the LTP.

It is instructive to compare the relative sensitivities of the three types of experiment with the aid of Fig. 14. The x-ray study of Ocko, Birgeneau, and Litster⁹ ceased to distinguish the difference between the order of a transition at $\Delta S/\Delta S^* \sim 1$ where a tricritical point is reported at 10% 10CB in 9CB. The adiabatic calorimetry measurements of Marynissen *et al.*⁶ failed at $\Delta S/\Delta S^* \sim 0.1$ where a tricritical point has been estimated at -3% 10CB in 9CB (i.e., 9CB is first order on the basis of adiabatic calorimetry measurements but its heat of transition is so small one cannot exclude it being second order). The dynamical measurements of Cladis *et al.*¹⁴ still see an apparently first-order transition for 8CB where $\Delta S/\Delta S^* \lesssim 0.01$.

VII. CONCLUSIONS

In this paper, we have shown that both the latent heat data obtained through adiabatic scanning calorimetry and independent interface velocity measurements for three series of mixtures can be fit remarkably well near the LTP by a crossover function consistent with a mean-field free-energy density that has a cubic term. The existence of such a term implies that in the regime studied, the N -Sm- A transition is at least weakly first order. The existence of such a cubic term had been predicted in 1974 by Halperin, Lubensky, and Ma,¹ and, to our knowledge, the analysis presented here gives the first detailed and quantitative evidence in support of this prediction. As regards the newly introduced dynamical method to test the order of a phase transition, we believe that the agreement of the theoretical results for the fluctuationless time-dependent Ginsburg-Landau equation (23) with experiment is better than one could reasonably hope for, in view of the various approximations made. Some of the points that in this regard deserve further study are the following.

(i) One prediction of simple Landau theory is that the dependence of the front velocity on direction of propagation should reflect that of the correlation length. In the 9CB-10CB mixtures, the anisotropy in the correlation length is close to an order of magnitude;⁹ however, no systematic anisotropy in the front velocity was detected in the experiment.¹⁴

(ii) The dynamics of the director fluctuations were ig-

nored in the above analysis of the front velocity. Can this approximation be justified?

(iii) Even for 8CB where the transition appears to be very weakly first order the visual contrast between the nematic- and smectic-*A* phases was sufficient to see the interface. Can the contrast (perhaps itself due to director fluctuations) be understood and perhaps even be used as an additional measure of the strength of the transition?

(iv) As discussed in Sec. V, our analysis of the temperature dependence of the interface velocity is only correct as long as the dynamics do not become diffusion limited. This certainly cannot be the case when the temperature jumps ΔT are much larger than L/c . For mixtures whose transition appears to be very weakly first order, we estimate on the basis of the parameters summarized in Table I that L/c is indeed small enough to be negligible (L/c might be smaller than 1 mK for pure 8CB, whereas typically $\Delta T \approx 20$ mK). However, for the mixtures that are strongly first order, L/c can become larger than ΔT . Depending on the sample geometry, the dynamical behavior might therefore show a crossover to a diffusion-limited behavior for these mixtures. This possibility has

not been explored systematically, however.

(v) One might wonder whether an imposed twist could have driven the transition weakly first order in the dynamical experiments. Although we do not believe this to be the case in view of the fact that the calorimetric data on the 9CB-10CB mixtures are in such good agreement with the dynamical measurements—which were performed in quite different sample geometries—this possibility deserves further study.

As regards the general applicability of the dynamical experiments, we finally note that its usefulness appears to be limited to phase transitions with a nonconserved order parameter. In the case in which the order parameter is a conserved quantity, the interface dynamics will typically be diffusion limited, so that it will be difficult to study the intrinsic interface dynamics.

ACKNOWLEDGMENTS

We are grateful to Ph. Nozières, B. I. Halperin, J. D. Litster, T. C. Lubensky, C. W. Garland, and J. Thoen for helpful and stimulating discussions.

- ¹B. I. Halperin, T. C. Lubensky, and S. K. Ma, Phys. Rev. Lett. **32**, 292 (1974); B. I. Halperin and T. C. Lubensky, Solid State Commun. **14**, 997 (1974).
- ²C. Dasgupta and B. I. Halperin, Phys. Rev. Lett. **47**, 1556 (1981); see also J. Bartholemew, Phys. Rev. B **28**, 5378 (1983).
- ³K. K. Kobayashi, Phys. Lett. A **31**, 125 (1970).
- ⁴W. McMillan, Phys. Rev. A **6**, 936 (1972).
- ⁵P. G. de Gennes, Solid State Commun. **10**, 753 (1972); Mol. Cryst. Liq. Cryst. **21**, 49 (1973); *The Physics of Liquid Crystals* (Clarendon, Oxford, 1974).
- ⁶J. Thoen, J. Marynissen, and W. van Dael, Phys. Rev. Lett. **52**, 204 (1984); H. Marynissen, J. Thoen, and W. van Dael, Mol. Cryst. Liq. Cryst. **124**, 195 (1985); J. Thoen, H. Marynissen, and W. van Dael, Phys. Rev. A **26**, 2886 (1982).
- ⁷M. A. Anisimov, V. P. Voronov, A. O. Kulkov, V. N. Petukhov, and F. Kholmudorov, Mol. Cryst. Liq. Cryst. **150b**, 399 (1987).
- ⁸For reviews of the experimental situation see, e.g., D. L. Johnson, J. Chim. Phys. Chim. Biol. **80**, 45 (1983) and J. D. Litster, Philos. Trans. R. Soc. London, Ser. A **309**, 145 (1983); cf. also T. C. Lubensky, J. Chim. Phys. Phys. Chim. Biol. **80**, 6 (1983); P. Pershan, *Structure of Liquid Crystal Phases* (World Scientific, Singapore, 1988).
- ⁹B. M. Ocko, R. J. Birgeneau, and J. D. Litster, Z. Phys. **62**, 487 (1986).
- ¹⁰D. Brisbin, R. deHoff, T. E. Lockhart, and D. L. Johnson, Phys. Rev. Lett. **43**, 1171 (1979); D. L. Johnson, C. F. Hayes, R. F. deHoff, and C. A. Schantz, Phys. Rev. B **18**, 4902 (1979).
- ¹¹C. W. Garland, G. B. Kasting, and K. J. Lushington, Phys. Rev. Lett. **43**, 1420 (1979).
- ¹²H. Marynissen, J. Thoen, and W. van Dael, Mol. Cryst. Liq. Cryst. **124**, 195 (1985).
- ¹³M. E. Huster, K. J. Stine, and C. W. Garland, Phys. Rev. A **36**, 2364 (1987).
- ¹⁴P. E. Cladis, W. van Saarloos, D. A. Huse, J. S. Patel, J. W.

Goodby, and P. L. Finn, Phys. Rev. Lett. **62**, 1764 (1989).

- ¹⁵The layer spacing in some compounds is about 1.3 times the molecular length. For example, the large dipole associated with cyanobiphenyl (CB) favors pairwise molecular associations with a distribution of lengths associated with a pair that is on the average longer than that of a single molecule. The smectic layer spacing is given by the average length of the ensemble of pairs. This specific detail affects only the values of the coefficients in the free-energy expansion.
- ¹⁶The derivation given here follows the one of HLM for the type-I regime. Since f' is quadratic in δn , one can of course also integrate out the director fluctuations directly. See, e.g., Ref. 18.
- ¹⁷P. Pfeuty and G. Toulouse, *Introduction to the Renormalization Group and to Critical Phenomena* (Wiley, New York, 1977). A pedagogical description of the HLM effect can be found in this book; a brief introduction to the connection between superconductors and the smectic-*A* phase can be found in Sec. 6.6 of G. Venkataraman, D. Sahoo, and V. Balakrishnan, *Beyond the Crystalline State* (Springer, New York, 1989).
- ¹⁸M. A. Anisimov, V. P. Voronov, E. E. Gorodetskii, V. E. Podneks, and F. Kholmudorov, Pis'ma Zh. Eksp. Teor. Fiz. **45**, 336 (1987) [JETP Lett. **45**, 425 (1987)].
- ¹⁹J. P. Hill, B. Keimer, K. W. Evans-Lutterodt, R. J. Birgeneau, and C. W. Garland, Phys. Rev. A **40**, 4625 (1989).
- ²⁰The simple estimate for B is $B \approx (k_0 \xi_{01})^3 \approx (\xi_1 / \xi_{||})^3 \approx 10^{-2}$. See Ref. 18.
- ²¹See, e.g., W. van Saarloos, Phys. Rev. A **37**, 211 (1988); **39**, 6367 (1989), and references therein.
- ²²J. Fineberg and V. Steinberg, Phys. Rev. Lett. **58**, 1332 (1987).
- ²³G. Ahlers and D. S. Cannell, Phys. Rev. Lett. **50**, 1583 (1983); see also M. Niklas, M. Lücke, and H. Müller-Krumbhaar, Phys. Rev. A **40**, 493 (1989).
- ²⁴Our discussion of propagating interfaces applies equally well to front propagation near instabilities. In the language appropriate to such applications, first-order transitions corre-

spond to inverted or subcritical bifurcations, and second-order transitions to forward or supercritical bifurcations.

²⁵See Eqs. (6.1) and (6.3) of Ref. 21.

²⁶Using the ansatz discussed in Sec. IV of Ref. 21, it is easy to

show that the interface velocity for $E=0$, $B>0$, $C>0$ is $v=[B/(8CM)^{1/2}\tau]^{-1}[-1+3(1-4AC/B^2)^{1/2}]$. This gives $g(+\infty)=3$ in Eq. (27).